Available online at www.sciencedirect.com
SCIENCE DIRECT®
Journal of Fluorine Chemistry 126 (2005) 241–250
JOURNAL OF FLUORINE CHEMISTRY
www.elsevier.com/locate/fluor

Novel fluorinated block copolymer architectures fuelled by atom transfer radical polymerization

Katja Jankova, Søren Hvilsted*

Danish Polymer Centre, Department of Chemical Engineering, Technical University of Denmark, Building 423, DK-2800 Kgs. Lyngby, Denmark

Received 2 June 2004; received in revised form 19 October 2004; accepted 8 November 2004
Available online 10 December 2004

Abstract

Block copolymers based on poly(pentafluorostyrene), PFS, in various numbers and of different lengths, and polystyrene are prepared by atom transfer radical polymerization (ATRP). Di- and triblock copolymers with varying amounts of PFS were synthesized employing either 1-phenylethylbromide or 1,4-dibromoxylene as initiators for ATRP. Diverse bromo(ester) (macro)initiators were also devised and involved in the formulation of fluorinated pentablock as well as amphiphilic triblock copolymers with a central polyether segment. Amphiphilic star-shaped fluoropolymers, hydrophobic fluorinated nanoparticles, or segmented fluorinated star-shaped block copolymers are further designed by use of different multifunctional initiators. The composition of the novel materials with PFS is determined by combination of SEC and ^{1}H NMR. Glass transition temperatures and thermal stabilities of the hydrophobic star-shaped PFSs on a six arm dipentaerythritol core are investigated in a wide range of molecular masses and further discussed.

Keywords: Pentafluorostyrene; ATRP; Bromoester macroinitiators; Block copolymers; Amphiphilic; Contact angle; Polyether blocks; Dipentaerythritol; Star-shaped polymers; Fluorinated nanoparticles

1. Introduction

Fluorinated polymers have always attracted significant attention due to high thermal stability, excellent chemical resistance, superior oil and water repellence or low flammability in addition to low refractive indexes [1]. Additionally, thin films of fluorinated polymers have recently been researched for low optical loss to be exploited in wave-guiding devices [2–5]. Also, low permittivity or low dielectric constants [6] are desirable properties for the optics and electronics industries. Furthermore, amphiphilic fluorine containing polymers appear to have a considerable potential as electrolyte materials for Li^+ conductivity in solid-state lithium-ion polymer battery applications [7,8]. Other recent, notable applications of fluoropolymers are in the form of block copolymers for generation of low-energy surfaces [9–19] or as surface-modified membranes [20].

Most fluorinated block copolymers with well-defined structures applied for generation of low-energy surfaces are either polystyrene based and initially prepared by living anionic polymerization [11,12,14–16,18,19] or poly(butyl methacrylate-*co*-perfluoroalkyl acrylate) [17] synthesized by atom transfer radical polymerization (ATRP). In addition, block copolymers with poly(ethylene oxide) and poly(perfluoroalkyl methacrylate) [21–23] have been prepared by ATRP. 2-Perfluoroalkyl containing initiators were likewise employed in ATRP of copolymers [24,25]. Low critical surface tensions have also been determined in fluorinated poly(amide urethane) block copolymers with fluorinated side chains prepared from diacid chlorides [9,10]. In the styrene based polymers the fluorination was obtained by functionalization of polystyryllithium and subsequent Williamson reactions [14,15], by deprotection of poly(4-*tert*-butyldimethylsiloxyloxystyrene) followed by William-

* Corresponding author. Tel.: +45 45252965; fax: +45 45882161.
E-mail address: sh@kt.dtu.dk (S. Hvilsted).

0022-1139/$ – see front matter © 2004 Elsevier B.V. All rights reserved.
doi:10.1016/j.jfluchem.2004.11.002

son reactions [15], or via oxidative hydroboration of isoprene blocks succeeded by esterification with perfluorinated acid chloride [11,12,14,19]. Finally, examples of TEMPO-mediated controlled radical polymerization of fluorinated alkoxymethylstyrene homo- [19] or block copolymers [26] also exist.

Most recently ATRP has proved to be the most rapidly growing area of polymer chemistry with numerous possibilities for polymerization of functional monomers in a controlled fashion, extended use of initiators with functional groups, and the potential polymer end group transformation [27]. Furthermore, ATRP has appeared as a valuable tool with great design flexibility awarding often full control of complex polymer composition, topology, and functionality including viable methods for preparation of molecular composites [28]. Thus, a number of monosubstituted styrenes, e.g. 4-fluoro- and 4-trimethylfluorostyrene, have been polymerized by ATRP [29]. That prompted us to investigate the polymerizability of the fully phenyl fluorinated styrene, 2,3,4,5,6-pentafluorostyrene (FS), by ATRP [30]; another brief report on FS polymerization by ATRP also exists [31]. The rewarding and fast polymerization of FS has been successfully followed by ATRP of 2,3,5,6-tetrafluoro-4-methoxystyrene (TFMS) [32,33]. Most recently, newly synthesized highly fluorinated fluoroalkoxy styrene monomers, 2,3,5,6-tetrafluoro-4-(2,2,3,3,3-pentafluoropropoxy)-styrene and 2,3,5,6-tetrafluoro-4-(2,2,3,3,4,4,5,5,6,6,7,7,8,8,8-pentadecafluoroctaoxy)styrene were found to produce polymers capable of forming low surface energy materials [34].

These findings open up new design avenues for preparation of novel fluorinated polymer materials. We here demonstrate how the potential of ATRP has been further exploited for synthesis of block copolymers (both hydrophobic and amphiphilic) with varying fluorine content. The application of multifunctional initiators based on hydroxyl compounds leads to the syntheses of novel fluorinated amphiphilic star-shaped materials that can be regarded as fluorinated nanoparticles. Finally, we elude to some possible applications of these novel materials that are currently under investigation.

2. Results and discussion

2.1. Block copolymers with varying fluorine content

The controlled characteristics of PFS and PTFMS were exploited in the preparation of a number of block copolymers [33]. The conservation of the bromine reactivity in the isolated homopolymers was indirectly proved through the efficient ability to act as macroinitiators (MIs). Fig. 1a illustrates a PFS-*b*-PS (**2**) block copolymer where the two end groups, 1-phenylethyl and bromine, originating from the initiator, 1-phenylethyl bromide, initially employed when the PFS macroinitiator was prepared, are shown. The block copolymers suffered only slight increases in the total polydispersity index (PDI = M_w/M_n) as compared with those of the initiating blocks. Furthermore, the applicability of the MIs in combination with the high reactivity of the monomers in this way provides a flexible tool for design of novel block copolymers. Moreover, the sequence of the blocks can easily be varied; in fact, among the mixtures of FS, TFMS and styrene (st.) all six possible combinations of block copolymers have been prepared. In practice, the decision on the block sequence adopted often depends on the solubility of the particular MI, which in turn also depends on the block length.

BAB type block copolymers have previously been synthesized in our group by ATRP using 1,4-dibromoxylene as the difunctional initiator [35]. The triblock copolymer in Fig. 1b, PFS-*b*-PS-*b*-PFS (**4**), was produced by two sequential

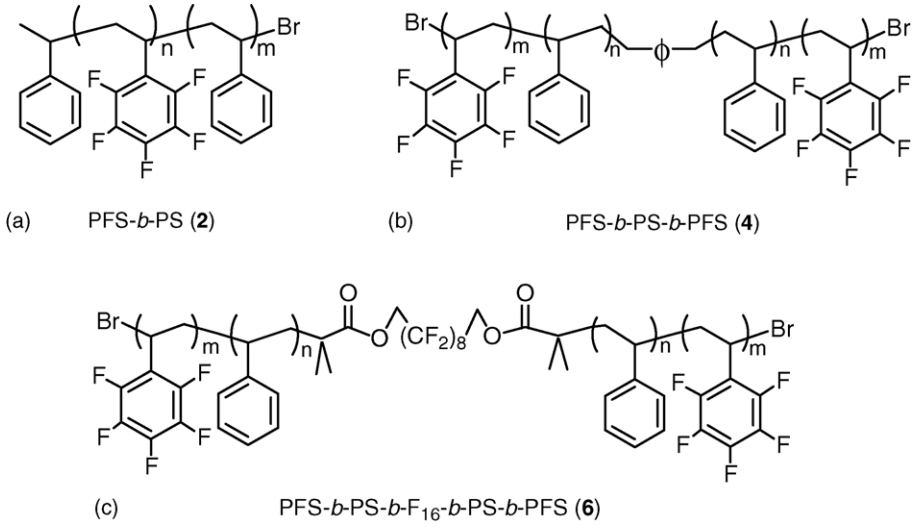

Fig. 1. Examples of diblock, triblock, and pentablock fluorocopolymers.

Table 1
Composition, molecular weights and contact angles of di-, tri-, and pentablock fluoropolymers

Polymer	M_n (RI)[a]	M_w/M_n (RI)[a]	M_n (LS)[a]	M_w/M_n (LS)[a]	PFS by ^{1}H NMR (wt.%)	Contact angle[b] (°)
PFS-Br (**1**)	10900	1.15				108[c]
PFS-*b*-PS (**2**)	21800	1.24			55	107
Br-PS-Br (**3**)	17400	1.14	21400	1.11		95[c]
PFS-*b*-PS-*b*-PFS (**4**)	25300	1.37	32200	1.34	19	
PS-*b*-F_{16}-*b*-PS (**5**-1)	6600	1.17				102
PS-*b*-F_{16}-*b*-PS (**5**-2)	11100	1.17				100
PFS-*b*-PS-*b*-F_{16}-*b*-PS-*b*-PFS (**6**-1)	19200	1.38			56	
PFS-*b*-PS-*b*-F_{16}-*b*-PS-*b*-PFS (**6**-2)	23900	1.36			58	

[a] RI: refractive index detector; LS: light scattering detector.
[b] Advancing contact angle of water droplet.
[c] Ref. [34].

ATRPs where the dibromo ends in the isolated Br-PS-Br (**3**) served as initiator for the subsequent polymerization with FS furnishing the triblock copolymer (**4**). Based on the PS calibration and the number average molecular weight (M_n) of the MI, the block copolymer composition listed in Table 1 was calculated by ^{1}H NMR as previously performed for diblock copolymers [30]. From these data the M_n of the block copolymer (**4**) was calculated by ^{1}H NMR to be 21,500. The examples presented in Fig. 1c, PFS-*b*-PS-*b*-F_{16}-*b*-PS-*b*-PFS (**6**-1 and **6**-2), are formally pentablock copolymers of the CBABC type, although the A block (F_{16} represents the fluorinated decanediol moiety) is very short. Nevertheless, in this manner it is possible to have three fluorinated blocks separated by PS blocks in the same copolymer. This type of block copolymer was also synthesized by two individual ATRP initially with St and then with FS. However, in this case a suitable initiator was first produced by converting a highly fluorinated decanediol, namely the 1H,1H′,10H,10H′-perfluorodecane-1,10-diol to the corresponding bromoester (A-block) as described in the following section, and outlined in Scheme 1 in case of the dihydroxypolyethers. Hereafter the procedure resembled the normal procedure for block copolymer synthesis. Finally, it should be noted that the fluorine content of block copolymers can easily be varied when PS constitutes one block.

Since the polymerizations perform in a controlled fashion, the fluorine content can to a certain extent be controlled through the original fluorine monomer to initiator ratio.

Continuous investigations of the fluorinated materials' surface properties were conducted by determination of the advancing contact angles (CA) of water drops on spin coated surfaces. The results of the CA determination listed in Table 1 show that the fluorine block introduced imparts higher hydrophobicity of the material surface as seen from the increase of the CA of **2** and **5** as compared with the non-fluorinated **3**. Even the small content of the central segment of 16 aliphatic fluorine atoms in **5**-2 corresponding to less than 4 wt.% of the polymer increases the CA of PS from 95 to 100°. The CA of the block copolymer **2** with 55 wt.% PFS reaches almost the CA of a homopolymer of FS (108° [34]). Thus it seems that the fluorinated blocks preferentially segregate at the air/film interface when spin coated, as confirmed recently for other fluorinated block copolymers [34].

2.2. Fluoropolymers with polyether blocks

A strategy for preparation of BAB triblock copolymers with a poly(ethylene glycol) (PEG) A, middle block flanked by PS end blocks (B) by ATRP was introduced already in 1998 by us [36,37]. The concept is based on quantitative

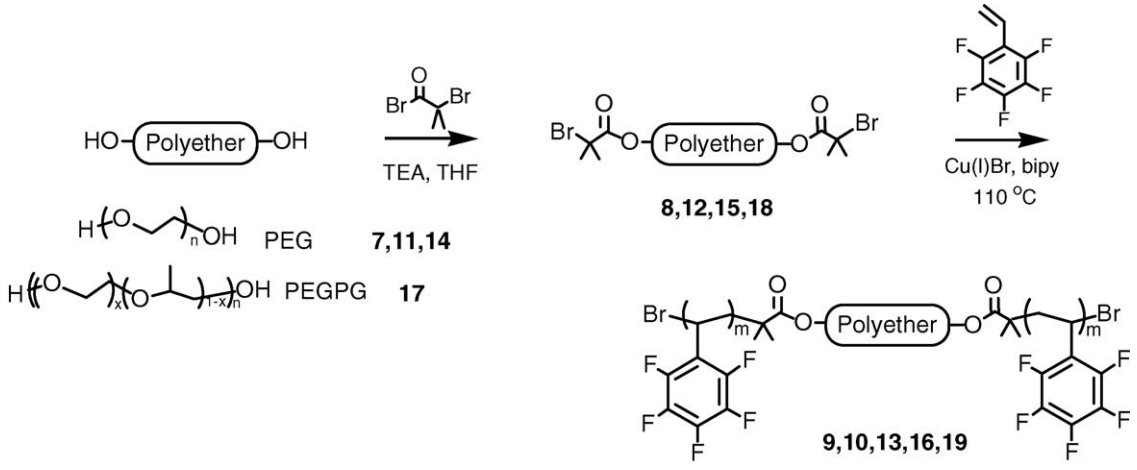

Scheme 1. Preparation of amphiphilic triblock fluorocopolymers by ATRP.

Table 2
Composition and molecular weights of amphiphilic triblock copolymers of PFS with a central polyether block

Polymer	$M_{n,SEC}$[a]	M_w/M_n[a]	PFS (wt.%)	$M_{n,NMR}$
PEG2 (**7**)	1900	1.02		
Br-PEG2-Br (**8**)	2400	1.02		
PFS-*b*-PEG2-*b*-PFS (**9**)	5300	1.05	80	9800
PFS-*b*-PEG2-*b*-PFS (**10**)	6200	1.05	84	12200
PEG5 (**11**)	4500	1.01		
Br-PEG5-Br (**12**)	4800	1.02		
PFS-*b*-PEG5-*b*-PFS (**13**)	7600	1.20	51	9500
PEG10 (**14**)	10300	1.12		
Br-PEG10-Br (**15**)	11000	1.16		
PFS-*b*-PEG10-*b*-PFS (**16**)	24300	1.20	39	17200
PEGPG (**17**)	9400	1.02		
Br-PEGPG-Br (**18**)	9600	1.05		
PFS-*b*-PEGPG-*b*-PFS (**19**)	15300	1.22	39	15800

[a] By SEC in THF employing PEG calibration.

conversion of the terminal hydroxyl groups in PEG to 2-bromo propionates. The bromine in this environment serves as an effective initiator for ATRP. The resulting bromine ester terminated PEG then performs as a difunctional MI employed in the preparation of PS-*b*-PEG-*b*-PS copolymers.

This strategy was adapted and exploited in the more recent work utilizing 2-bromoisobutyryl bromide for the design of triblock copolymers with PFS blocks as outlined in Scheme 1. A number of PEGs with M_ns from 2 to 10×10^3 (**7**, **11**, **14**) were employed as listed in Table 2. Additionally, a liquid, dihydroxy terminated random copolymer (**17**) of ethylene and propylene oxide (PEGPG with 74 wt.% PEG) with a molecular weight of nearly 10,000 was also used.

In all cases the quantitative conversion of the hydroxyl groups was verified by ^{1}H NMR spectroscopy. Furthermore, size exclusion chromatography (SEC) strongly implies that the rather low PDI (M_w/M_n) from the polyethers is preserved in the MIs (**8**, **12**, **15**, **18**). The ATRP with FS allowed PFS blocks, on the order of 39–84 wt.%, to be added to the polyether blocks (**9**, **10**, **13**, **16**, **19**) as determined by a combination of SEC and ^{1}H NMR. In addition, the SEC revealed PDIs < 1.22 for the triblock copolymers.

These amphiphilic triblock copolymers have very interesting material properties. For example PFS-*b*-PEGPG-*b*-PFS (**19**) is a good film forming material, probably due to a strong phase separation in which the PFS domains act as physical crosslinks. In fact, even a much lower PFS content on the order of 3–9 wt.% ensures the formation of an elastomeric material [38]. We believe that the molecular construction is quite similar to the thermoplastic elastomers where two PS outer blocks flank an elastomer central block. However, in this case an even stronger phase separation between the fluoropolymer blocks and the polyether segments is envisioned due to the strong amphiphilic character of the material. Furthermore, the polyether block in this material has demonstrated good Li^+ complexation when mixed with Li salts while the composite still maintains the favourable film forming properties. Moreover, this composite has demonstrated good Li^+ conductivity ($10^{-4.9}$ to $10^{-5.1}$ S cm^{-1} at 20 °C) over a viable temperature range (−40 to +100 °C) [38]. Additionally, it seems that in some instances the fluorinated blocks ensure good contact between the electrode materials and the electrolyte polymer. Consequently they appear as potential candidates for electrolyte materials in solid-state Li^+ polymer battery applications.

2.3. Fluorinated star-shaped polymers

A tetrafunctional MI, **21**, was prepared by reacting the star-shaped PEG, **20** (based on a pentaerythritol core) shown in Scheme 2 with 2-bromoisobutyryl bromide. Star-shaped block copolymers, *star*-PEG-*b*-PFS (**22**), with flanking outer PFS blocks were prepared by application of **21** for ATRP of FS (Scheme 2, Table 3).

The SEC traces of both star-shaped block copolymers (**22**) are completely shifted from those of **20** and **21** indicating that block copolymers were prepared. Based on the SEC calibration with PEG standards and M_n of **21**, the

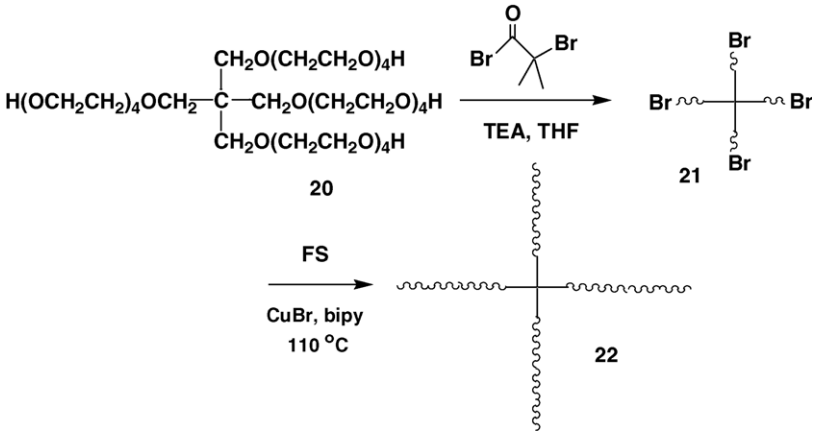

Scheme 2. The principle route for preparation of fluorinated amphiphilic star-shaped block copolymers by ATRP.

Table 3
Composition and molecular weights of amphiphilic tetra-arm star polymers

Polymer	Composition		Molecular weights		
	PEG (wt.%)[a]	PFS (wt.%)[a]	M_n[b]	M_w/M_n[b]	M_n[a]
Star-PEG (**20**)	83		940	1.04	
Star-PEG-*b*-PFS (**22**-1)	10	88	5700	1.30	7300
Star-PEG-*b*-PFS (**22**-2)	8	91	6800	1.30	9000

[a] By ^{1}H NMR.
[b] By SEC with PEG calibration.

block copolymer compositions listed in Table 3 were calculated by ^{1}H NMR [38]. Even as little as 8–10 wt.% of the hydrophilic part render the block copolymers (**22**) amphiphilicity resulting in formation of micelles in THF/water solutions. The micellization behaviour of (**22**) is under investigation.

Exploitation of multifunctional ATRP initiators initially based on the hydroxyl functions has been extended further to include compounds that would provide principally spherical growth to form star-shaped block copolymers. Scheme 3 illustrates the strategy starting from dipentaerythritol (**23**) that is quantitatively converted to a hexafunctional ATRP initiator (**24**) by the synthetic approach developed for PEG. The remarkable symmetry of this rather large molecule, **24**, is reflected by the simplicity of both the ^{1}H and ^{13}C NMR spectra [39]. Furthermore, a SEC analysis performed on an OligoSEC column dedicated to relatively small macromolecules strongly implies that **24** is a pure compound.

24 was employed as initiator in a bulk ATRP of FS at 110 °C as shown in Scheme 3. Achieving high conversion of FS by ATRP with **24** in bulk is not a problem, however, the SEC traces are four to six modal and M_w/M_n is high. This is probably caused by termination of each growing arm at certain, but different stages due to the viscosity of the system

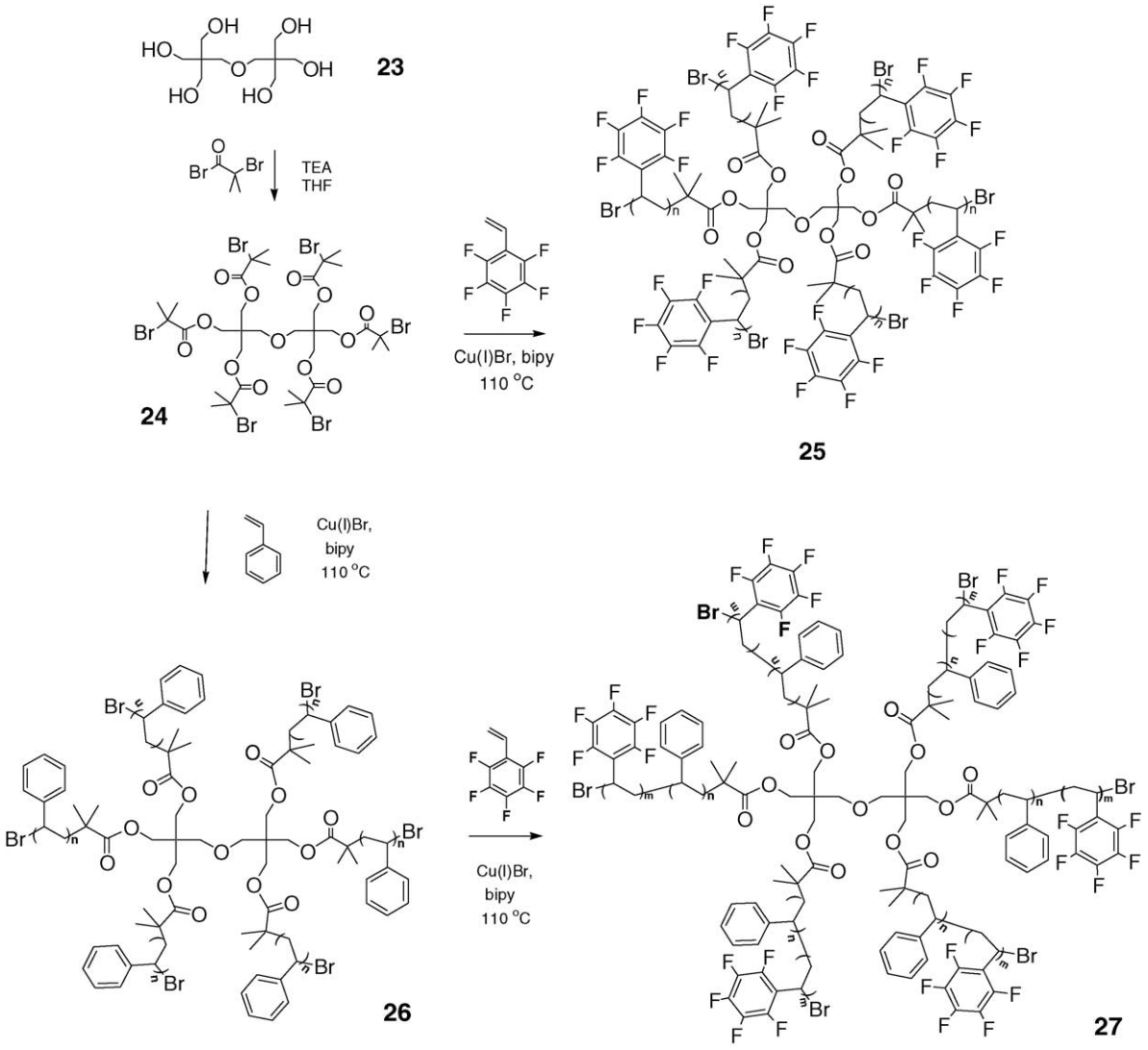

Scheme 3. The principal route for preparation of hexa-arm star fluoro and segmented block copolymers by ATRP.

Table 4
Molecular weights, glass transition temperatures, T_gs, and thermal stabilities of hexa-arm *star*-fluoropolymers of PFS prepared by ATRP

Polymer[a]	M_n (RI)	M_w/M_n	M_n (LS)	T_g (°C)	TGA[b] first step (%)	TGA[c] residue (%)
25-1	2600	1.08	–	56	25.8	6.2
25-2	4050	1.18	–	75	20.3	4.6
25-3	4400	1.10	–	76	19.7	4.5
25-4	5050	1.13	–	82	16.3	3.8
25-5	7200	1.21	–	82	12.1	2.9
25-6	8200	1.11	24000	–	–	–
25-7	10800	1.19	–	87	11.9	2.5
25-8	11400	1.10	27000	–	–	–
25-9	21300	1.25	49500	99	–	–
25-10[d]	67400	1.50		99	2.2	1.1

[a] Prepared by ATRP in bulk at 110 °C with the catalytic system CuBr/bipy using 0.03 mmol **24** and FS: **24** = 460 (**25**-1) for 2 min and (**25**-2 to **25**-4) for 5 min; 1100 (**25**-5 to **25**-7) and 1600 (**25**-8) for 7 min to 1–3% conversion.
[b] Weight loss of the sample during the first step in the temperature range 277–350 °C.
[c] Weight residue of the sample at 500 °C.
[d] Prepared as above (see footnote a) in 10% xylene solution of FS to 18% conversion with FS: **24** = 1700 for 45 min.

at higher conversions. Different shapes of the SEC traces are observed when the ATRP is performed either in bulk to only 10–20% conversion or in solutions of xylene, diphenyl ether or THF. The polymers produced in this way show three modal distributions with both a low and a high molecular weight shoulder in addition to the main peak. The low molecular weight shoulder is very small and presumably due to an early termination of one or more growing arms of the stars. While the high molecular weight analogue is probably caused by star-star coupling, since the corresponding, calculated M_n value is at least twice as high as the one resulting from the main peak. Such a polymer with M_n of 67,400 and PDI = 1.50 is **25**-10 listed in Table 4. It is produced in 10% solution of FS in xylene to 18 wt.% conversion and contains a slightly visible low molecular weight shoulder and a high molecular weight peak (M_n = 108,900; PDI = 1.28) with lower intensity than the main peak with M_n of 43,100 and PDI = 1.04. Other attempts to avoid these side reactions failed. Neither lower temperatures (down to 85 °C) nor changing the ligand have helped to increase the control. Nevertheless, a number of well-defined hexa-arm *star*-PFSs with different, but increasing M_ns were prepared and presented in Table 4. They were obtained by ATRP of FS in bulk at 110 °C to low conversions (1–3%) employing the catalytic system Cu^IBr:bipy. Beyond this limit of conversion for FS, irreversible recombination reactions between stars became visible by SEC, while this happened much later (at around 23% conversion) when polymerizing St [39]. A SEC trace of the hexa-arm *star*-PFS polymer (**25**-8) in THF prepared in this manner is provided in Fig. 2. In this case the narrow peak shape of the SEC is observed. Furthermore, we interpret the shape of the trace and the low polydispersity index as an indication that all six arms grew simultaneously at approximately the same rate with little or no crosslinking due to radical coupling reactions. However, star polymers of high functionality are known to exhibit smaller radii of gyration and therefore lower viscosity than linear ones. Thus, providing numbers for M_n based on linear PS calibration appears meaningless. The M_n figures reported in Tables 1 and 4 obtained by LS are preliminary results that need further elaboration; however, they seem to be more realistic values. The hexa-arm fluoropolymers synthesized can be considered as fluorinated nanoparticles. Thus, a novel route for synthesis of fluorinated nanoparticles has been devised.

The T_g of the *star*-PFSs increases from 56 °C for sample **25**-1 with M_n of 2600 to 87 °C for **25**-7 with M_n of 10,800 and levels off at M_n of 21,300 (**25**-9) to 99 °C. A similar dependence of T_g on molecular weight has previously been observed by us for linear PFSs [30].

The arms of the *star*-PFSs are connected to the core via ester linkages. In principle, this allows for cleavage by hydrolysis which could provide a possibility to analyze the size and molecular weight distribution of the cleaved linear chains. Several of the *star*-PFSs prepared were subjected to hydrolysis under basic conditions as in the case of *star*-PSs [39]. Hydrolysis of the esters was attempted by refluxing a THF solution of the star polymers with KOH (in ethanol) [40,41]. To our surprise no cleavage was observed even after several weeks of hydrolysis. This was the first indication that

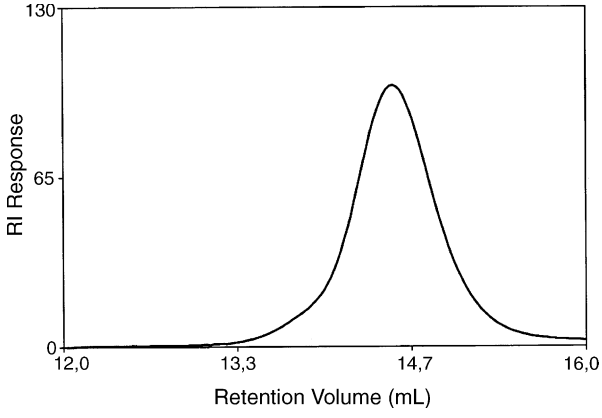

Fig. 2. SEC of hexa-arm *star*-PFS (**25**-8).

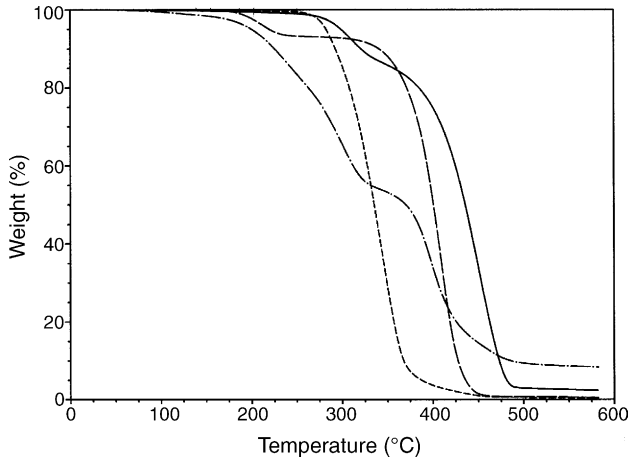

Fig. 3. TGA traces of the total weight loss of **23** (- - -), **24** (– · – ·), **25**-5 (—), and **26** (– – –).

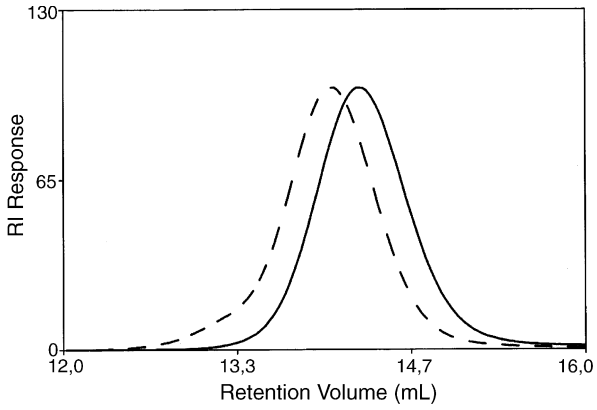

Fig. 4. SEC of hexa-arm star-PS, **26**-1 (—) and hexa-arm *star*-PS-*b*-PFS, **27**-1 (– – –).

the ester bonds are shielded and protected by the hydrophobic FS and therefore inaccessible to hydrolysis. Additionally, the H-containing groups in the core of the *star*-PFSs could not be seen by ^{1}H NMR.

In order to study further this fact the thermal stability of the *star*-PFSs synthesized was investigated by thermogravimetric analysis (TGA) in a N_2 atmosphere. Fig. 3 shows the representative TGA curves of the total weight loss for **23**, **24**, **25**-5, and a *star*-PS (**26**) with M_n = 10,000 (PDI = 1.13) prepared by ATRP with the same MI (**24**). The thermostability of **23** and **24** appears quite different. The degradation of **23** starts at 260 °C, while the main degradation of **24** already starts at 180 °C, and occurs in two steps. The first step lasts until around 330 °C where the resulting weight loss of 54–55%, seems to correspond to the scission of the ester linkages in **24**. The second step is probably connected with degradation of condensation species formed in the first step but with higher thermostability than those of pure **23**, as evidenced from the overlay in Fig. 3. Also, all *star*-PFSs (**25**) investigated show two steps of the weight loss—one starting at around 277–350 °C, suggesting that a thermal degradation of the star polymers involving the core happens prior to the main polymer itself. This behaviour was additionally found for *star*-PSs, but the first degradation step initiates almost 100° lower, at around 180 °C. The extent of the first step for both **25** and **26** increases with decreasing M_n of the star polymer, which correlates with the amount of the aliphatic part introduced from **24.** The weight losses of the *star*-PFSs samples in the range 277–350 °C are presented in Table 4. At the same time **24** reveals a 9.4% weight residue at 500 °C while linear PFSs or PSs produced by ATRP do not leave any residues [30]. For example the weight loss from 277 to 350 °C decreases from 25.8 to 2.2% with increasing the M_n of the *star*-PFS from 2600 (**25**-1) to 67,400 (**25**-10), respectively, while the amount of the residue at 500 °C decreases accordingly from 6.2 to 1.1 (Fig. 3, Table 4). These observations reveal that the thermal degradation of *star*-PFSs involves as a first step the core scission as in case of *star*-PSs. Nevertheless, FS still renders higher thermostability to the produced star polymers as in the case of the linear ones [30].

The macroinitiator concept as the basis for a copolymer was also pursued with the star polymers. However, the fluoropolymer blocks should stay at the surface of the nanoparticles in order to benefit mostly from the fluoropolymer characteristics. Therefore a hexa-arm *star*-PS (**26**) was first prepared by use of the MI (**24**) in accordance with the procedure outlined in Scheme 3. The SEC trace of the isolated hexa-arm *star*-PS (**26**-1) is shown in Fig. 4. The shape of the trace has strong resemblance to that of the hexa-arm *star*-PFS presented in Fig. 2. The SEC analysis based on PS calibration suggests a M_n of 11,600 (RI) and 16,700 (LS) with M_w/M_n of 1.12–1.13.

It should be noted that although the SEC analysis is performed with PS calibration we only consider the M_n value indicative due to the spherical shape. On the other hand, the polydispersity index of 1.12 is again believed to reflect the controlled growth of the six PS arms with virtually no chain coupling. The isolated hexa-arm *star*-PS (**26**-1) was then used as a hexafunctional MI for a new ATRP procedure with FS. The overlayed SEC trace of one of this block copolymer, **27**-1, in Fig. 4 strongly suggests within the reliability of the method that also the second PFS layer is grown in a controlled fashion. In this way the PS core blocks of the

Table 5
Compositions and molecular weights of hexa-arm *star*-PS and segmented *star*-PS-*b*-PFS copolymers prepared by ATRP

Polymer	M_n (PDI) (RI)	M_n (PDI) (LS)	PFS (wt.%) (NMR)	$M_{n,NMR}$
26-1	11600 (1.12)	16700 (1.13)	0	–
27-1	14300 (1.27)	33200 (1.15)	71	40000
27-2	20200 (1.27)	–	89	105000
26-2	12400 (1.12)	–	0	–
27-3	15500 (1.14)	–	64	34500
26-3	19200 (1.17)	34000 (1.18)	0	–
27-4	33200 (1.14)	–	–	–

hexa-arm *star*-PS (**26**) could be surrounded by PFS blocks in a corona, thus forming segmented, block copolymers. As PS and PFS show similar glass transition temperatures (~100 °C [30]) for the segmented block copolymer, **27**-1, only one T_g of 91 °C with a broad transition was found, where the MI **26**-1, itself had T_g of 82 °C. Table 5 lists 2 other *star*-PS MIs, **26**-2 and **26**-3, and the corresponding star block copolymers **27**-3 and **27**-4 prepared in this manner.

3. Conclusions

We have attempted to demonstrate the versatility of ATRP to enable preparation of different, novel fluorinated polymer architectures based on the fully phenylfluorinated styrene monomer, FS. The attractive ability of the resulting PFS homopolymers to function as macroinitiators was further exemplified by the facile preparation of linear diblock copolymers with PS. Also triblock copolymers were prepared by use of 1,4-dibromoxylene as the difunctional initiator. Thus, varying amounts of FS can easily be incorporated in the copolymers when used in combination with St. A short, fluorinated dibromoester could be used as ATRP initiator for St. The fluorinated copolymers enrich the surface of thin films resulting in an increased advancing water contact angle of 107° (for PFS-*b*-PS) and 100° (for PS-*b*-F_{16}-*b*-PS). These, as well as our former results with 4-substituted fluoroalkoxy side chains PFSs (CA of 117–122° [34]) strongly suggest that the fluorinated blocks in the investigated fluorinated copolymers of PS migrate to the open film surface and create low surface energy films.

Multiblock copolymers based on different difunctional bromine initiators, e.g. 1,4-dibromoxylene, were likewise synthesized. Even more important is the possible quantitative bromoester derivatization of compounds with two or more hydroxyl groups. Thus, the short fluorinated dibromoester gave rise to a pentablock copolymer with alternating fluorinated and PS blocks. Various hydroxyl-terminated polyethers of different lengths were converted to macroinitiators according to this concept and a number of triblock copolymers with PFS end blocks were prepared. These amphiphilic block copolymers have very interesting material properties such as good Li^+ complexation while preserving excellent film forming capability. Since the Li^+ conductivity is high, such materials seem interesting for solid-state electrolyte applications in batteries. The flexibility of the initiator concept could be broadened to the synthesis of a tetrafunctional hydrophilic MI based on a *star*-PEG, which was extended to amphiphilic *star*-PEG-*b*-PFS copolymers. A hexafunctional MI with a dipentaerythritol core was the basis for preparation of a number of hydrophobic hexa-arm star fluoropolymers. Thereby a route for preparation of novel fluorinated nanoparticles has been devised. These nanoparticles may consist entirely of the fluoropolymer PFS or have a PS core surrounded by a PFS corona. Even though the thermal degradation involves first a core scission, PFS still renders higher thermal stability to the produced star polymers as in the case of the linear analogues.

4. Experimental

4.1. Materials

Styrene, (Sigma–Aldrich) and 2,3,4,5,6-pentafluorostyrene, FS (Fluorochem Limited, UK) were liberated from the stabilizer and vacuum distilled before use. CuBr, 2,2′-bipyridine (bipy) and 1,4-dibromoxylene (all from Sigma–Aldrich) were employed as received. THF and triethylamine (TEA) were distilled from CaH_2. The polyethers and glycols were dried either by azeotropic distillation with toluene (1H,1H′,10H,10H′-perfluorodecane-1,10-diol from ABCR-Germany; *star*-PEG, PP150 from Perstorp Polyols, Sweden) or at 180 °C for several hours (dipentaerythritol, from Perstorp Polyols, Sweden).

4.2. Synthesis

The dried polyols were converted to MI by reaction with 2-bromoisobutyryl bromide catalyzed by TEA in anhydrous THF [36]. In a typical ATRP procedure [30] an appropriate amount of the MI was dissolved either in the monomer or in xylene in a Schlenk tube and the necessary amounts of FS, CuBr, and bipy in order to reach $M_{n,target}$ ($M_{n,target} = [FS]_0/[MI]_0$ at 100% conversion) were added. The molar ratio of initiating groups:CuBr:bipy was kept 1:1:2. After three freeze-thaw cycles, the polymerization tube was immersed in a preheated oil bath at 110 °C. The polymerization was stopped after the appropriate time by transferring the tube to a cooling bath. The polymer solutions were then filtered, if necessary after dilution with THF, and precipitated in methanol. When the ATRP's of FS were run until low conversions the big excess of the monomer was vacuum distilled prior to dilution with THF and precipitation. Conversions of FS in the homo- and block copolymers formed were determined gravimetrically after vacuum drying.

4.3. Analysis: NMR spectroscopy

The macroinitiators and the block copolymers were characterized by ^1H NMR, using a Bruker 250 MHz spectrometer and DMSO-d_6 or $CDCl_3$ as solvents. ^{19}F NMR in C_6F_6 constitutes only of three broad peaks for the di- and triblock copolymers of PFS and PS at −154.6 ($2F_{ar}$), −147.6 ($1F_{ar}$) and −137.0 ($2F_{ar}$) ppm as for the PFS homopolymer. The composition of the various block copolymers of PFS with PS or polyethers (Tables 1 and 5) was determined therefore by ^1H NMR in a similar way as published before [30,38]. Ratio analysis of the area of aliphatic protons (from both PFS and PS main chains, 1.8–3.3 ppm) and the area of the aromatic protons (from only PS,

6.5–7.4 ppm) was used. The content of PFS, w_{PFS} (in wt.%), in the block copolymer with PEG presented in Table 2 was calculated by $w_{PFS} = 194A_{PFS}/(194A_{PFS} + 33A_{PEG})$, where A_{PFS} is the area of the aliphatic protons of the PFS segment between 1.8 and 2.9 ppm and A_{PEG} is the area of the PEG protons around 3.6 ppm. The amount of PFS in the PEGPG block copolymers was determined in a similar way. The composition of the *star*-PEG, PP 150, is calculated from the mass of the 15 ethylene oxide units as compared to the total mass of 800 g mol^{-1}, given by the producer. The content of ethylene oxide in mol% in the amphiphilic PP 150 based star-shaped block copolymers is calculated by the ratio of the area for the 15 PEG units (60 protons) at 3.2–4.1 ppm as compared with its sum of the area for the PFS protons (1.5–2.9 ppm).

The $M_{n,NMR}$ of the polyether based block copolymers was calculated as:

$$M_{n,NMR} = \frac{M_{n,SEC}^{polyether}}{(100 - w_{PFS})/100} + 150 f_n,$$

while the $M_{n,NMR}$ of the amphiphilic star-shaped block copolymers was determined as:

$$M_{n,NMR} = \frac{660}{w_{PEG}/100} + 150 f_n + 132,$$

where 150 is the mass of the initiating Br-ester end group, 660 is the mass of 15 ethylene oxide units, w_{PEG} is the wt.% of 15 ethylene oxide units, and f_n is the number-average functionality of the starting polyether (2 for PEGs and PEGPG, and 4 for *star*-PEG).

4.3.1. SEC analysis

Molecular weights were determined by SEC employing a Viscotek 200 instrument equipped with a PLguard and 2 PLgel mixed D columns in series from Polymer Laboratories (PL). Measurements were performed in THF at room temperature with a 1 mL min^{-1} flow and RI detection; molecular weights were calculated using either PS in the range 7×10^2 to 4×10^5 or PEG narrow molecular weight standards (10^2 to 6×10^4) from PL and the TriSEC^{TM} Software.

4.3.2. DSC analysis

Thermal analyses were executed with a differential scanning calorimeter DSC Q1000 from TA Instruments in a temperature range of −100 to 200 °C at a heating rate of 10 °C min^{-1} under nitrogen. The glass transition temperature (T_g) was determined automatically by the instrument from the second heating trace and is reported as the midpoint of the thermal transition.

Thermal degradation was investigated by TGA performed with a TGA Q500 from TA Instruments recording the total weight loss on approx. 10–12 mg samples from room temperature to 600 °C at a rate 10 °C min^{-1} in a nitrogen flow of 90 mL min^{-1}.

Acknowledgements

Aage and Johanne Louis-Hansen's Foundation (DK) and Materials Research, Danish Research Agency is gratefully acknowledged for financial support. We additionally thank Sokol Ndoni, Risø National Laboratory, DK, for performing the SEC light scattering (LS) analyses. Perstorp Polyols, SE, is acknowledged for kindly supplying dipentaerythritol and PP150.

References

[1] J. Nieratschker, Kunststoffe 89 (1999) 130–134.
[2] H.-J. Le, M.-H. Lee, M.C. Oh, J.-H. Ahn, S.G. Han, J. Polym. Sci., Part A: Polym. Chem. 37 (1999) 2355–2361.
[3] C. Pitois, S. Vukmirovic, A. Hult, D. Wiesmann, M. Robertsson, Macromolecules 32 (1999) 2903–2909.
[4] J.-P. Kim, W.-Y. Lee, J.-W. Kang, S.-K. Kwon, J.-J. Kim, J.-S. Lee, Macromolecules 34 (2001) 7817–7821.
[5] C. Pitois, D. Wiesmann, M. Lingren, A. Hult, Adv. Mater. 13 (2001) 1483–1487.
[6] L.M. Han, R.B. Timmons, W.W. Lee, Y.C. Chen, Z. Hu, J. Appl. Phys. 84 (1998) 439–444.
[7] P. Gavelin, P. Jannasch, B. Wesslén, J. Polym. Sci., Part A: Polym. Chem. 39 (2001) 2223–2232.
[8] P. Gavelin, P. Jannasch, I. Furó, E. Pettersson, P. Stilbs, D. Topgaard, O. Söderman, Macromolecules 35 (2002) 5097–5104.
[9] T.M. Chapman, R. Benrashid, K.G. Marra, J.P. Keener, Macromolecules 28 (1995) 331–335.
[10] T.M. Chapman, K.G. Marra, Macromolecules 28 (1995) 2081–2085.
[11] D.R. Iyengar, S.M. Perutz, C.-A. Dai, C.K. Ober, E.J. Kramer, Macromolecules 29 (1996) 1229–1234.
[12] J. Wang, G. Mao, C.K. Ober, E.J. Kramer, Macromolecules 30 (1997) 1906–1914.
[13] J. Wang, C.K. Ober, Macromolecules 30 (1997) 7560–7567.
[14] A. Böker, K. Reihs, J. Wang, R. Stadler, C.K. Ober, Macromolecules 33 (2000) 1310–1320.
[15] K. Sugiyama, T. Nemoto, G. Koide, A. Hirao, Macromol. Chem. 181 (2002) 135–153.
[16] A. Hirao, G. Koide, K. Sugiyama, Macromolecules 35 (2002) 7642–7651.
[17] K. Li, P. Wu, Z. Han, Polymer 43 (2002) 4079–4086.
[18] L. Andruzzi, E. Chiellini, G. Galli, X. Li, S.H. Kang, C.K. Ober, J. Mater. Chem. 12 (2002) 1684–1692.
[19] A. Böker, T. Herweg, K. Reihs, Macromolecules 35 (2002) 2937–4929.
[20] T. Miyata, H. Yamada, T. Uragami, Macromolecules 34 (2001) 8026–8033.
[21] H. Hussain, H. Budde, S. Höring, K. Busse, J. Kressler, Macromol. Chem. Phys. 203 (2002) 2103–2112.
[22] H. Hussain, K. Busse, J. Kressler, Macrolmol. Chem. Phys. 204 (2003) 936–946.
[23] K.T. Lim, M.Y. Lee, M.J. Moon, G.D. Lee, S.-S. Hong, J.L. Dickson, K.P. Johnston, Polymer 43 (2002) 7043–7049.
[24] S. Perrier, S.G. Jackson, D.M. Haddleton, B. Améduri, B. Boutevin, Macromolecules 36 (2003) 9042–9049.
[25] B. Améduri, B. Boutevin, Well-Architectured Fluoropolymers: Synthesis, Properties and Applications (F-Telomers, Telechelics, and Alternated, Block and Graft Copolymers), Elsevier, Amsterdam, 2004.
[26] P. Lacroix-Desmazes, B. Boutevin, D.K. Taylor, J.M. DeSimone, Polym. Preprints 43 (2) (2002) 285–286.
[27] V. Coessens, T. Pintaur, K. Matyjaszewski, Prog. Polym. Sci. 26 (2001) 337–377.

[28] K. Matyjaszewski, J. Xia, Chem. Rev. 101 (2001) 2921–2990.
[29] J. Qiu, K. Matyjaszewski, Macromolecules 30 (1997) 5643–5648.
[30] K. Jankova, S. Hvilsted, Macromolecules 36 (2003) 1753–1758.
[31] J.A. Johnson, C.S. Gudipati, K.L. Wooley, Polym. Preprints 44 (2) (2003) 238.
[32] S. Hvilsted, S. Borkar, L. Abildgaard, V. Georgieva, H.W. Siesler, K. Jankova, Polym. Preprints 43 (2) (2002) 26–27.
[33] S. Hvilsted, S. Borkar, H.W. Siesler, K. Jankova, Novel fluorinated polymer materials based on 2,3,4,5-tetrafluoro-4-methoxystyrene, in: K. Matyjaszewski (Ed.), Advances in Controlled/Living Radical Polymerization, ACS Symposium Series, vol. 854, American Chemical Society, Washington, DC, 2003, pp. 236–249 (Chapter 17).
[34] S. Borkar, K. Jankova, H.W. Siesler, S. Hvilsted, Macromolecules 37 (2004) 788–794.
[35] B. Gao, X. Chen, B. Ivan, J. Kops, W. Batsberg, Macromol. Rapid Commun. 18 (1999) 1095–1100.
[36] K. Jankova, X. Chen, J. Kops, W. Batsberg, Macromolecules 31 (1998) 538–541.
[37] K. Jankova, J.H. Truelsen, X. Chen, J. Kops, W. Batsberg, Polym. Bull. 42 (1999) 153–158.
[38] K. Jankova, P. Jannasch, S. Hvilsted, J. Mater. Chem. 14 (2004) 2902–2908.
[39] K. Jankova, M. Bednarek, S. Hvilsted, J. Polym. Sci., Part A: Polym. Chem., submitted for publication.
[40] S. Angot, K.S. Murthy, D. Taton, Y. Gnanou, Macromolecules 31 (1998) 7218–7225.
[41] A.P. Narrainen, S. Pascual, D.M. Haddleton, J. Polym. Sci., Part A: Polym. Chem. 40 (2002) 439–450.